Journal of Crystallographic and Spectroscopic Research, Vol. 22, No. 5, 1992

Molecular and crystal structure of 2-amino-4-(tricyclo[3.3.1.1.3,7]decyl-1)-6-N-methyl-piperazino-1,3,5-triazine

S. J. Hamodrakas,*[,1] A. Hempel,[2] N. Camerman,[2] F. P. Ottensmeyer,[1] P. Tsitsa,[3] E. Antoniadou-Vyzas,[3] and A. Camerman[4]

Received October 14, 1991; accepted January 29, 1992

The crystal and molecular structure of the title compound has been determined by X-ray diffraction. The compound crystallizes in the rhombohedral space group $R3$ with $a = b = c = 17.804(9)$ Å, $\alpha = \beta = \gamma = 116.48(2)°$ and $Z = 6$. The structure was solved by direct methods and a full-matrix least-squares refinement converged to a final $R = 0.061$ for 1922 unique reflections. The adamantyl moiety is statically disordered in the crystal structure, and adopts two conformations related by the rotation of approximately 60° about the C(4)—C(9) bond. A hydrogen bond between N(7) · · · N(21) arranges molecules into hexamers stacked along the threefold axis and provides for empty hydrophobic channels bounded by the adamantyl groups.

Introduction

Dihydrofolate reductase [5,6,7,8-tetrahydrofolate: NADP+ oxidoreductase (EC 1.5.1.3); DHFR], an enzyme which reduces dihydrofolic to tetrahydrofolic acid, is a protein of central importance in biochemistry and medicinal chemistry (Blakley, 1969). It is used as a target for several antibacterial and antineoplastic (antitumor) drugs. The antibacterial activity of these drugs is due to selective inhibition of the enzyme from species to species (Baccarani *et al.*, 1982; Hitchings and Smith, 1980). Unfortunately, the molecular mechanism of selective inhibition is not yet known, despite extensive efforts.

The findings that diamino-s-triazines interfere with folic acid metabolism stimulated research on the antifolate activity of this class of compounds, which have shown promise in cancer chemotherapy (Modest *et al.*, 1952). A conclusion drawn from these studies is that for several antifolates the extent of their uptake, their growth inhibitory potency on tumor cells, as well as their affinity to DHFR correlates with lipophilicity (Greco and Hakala, 1980).

In the course of our investigation on adamantane ring bearing compounds (Antoniadou-Vyzas and Foscolos, 1986; Garoufalias *et al.*, 1988) we considered likely that this group attached on a triazine ring could make effective use of the enzyme hydrophobic cavity. In addition, the absence of any information on amino-substituted analogs as antifolates, in contrast to the plethora of similar information on the diamino-derivatives, prompted us to attempt substitution on the 6-amino nitrogen of the triazine molecule. Therefore, possible DHFR inhibitors of the general types I and II (Scheme 1) have been synthesized as possible antitumor, antibacterial, and antifungal agents.

All compounds are currently being tested for DHFR-binding affinity and pharmacological properties (Tsitsa *et al.*, in preparation). In order to understand the observed variation in biological activity and compare structure and binding with other antifolate ligands, crys-

*To whom correspondence should be sent at: Department of Biology, University of Athens, Panepistimiopolis, Athens 15701, Greece.
[1]Department of Medical Biophysics, University of Toronto, Toronto Ontario, M4X 1K9, Canada.
[2]Department of Biochemistry, University of Toronto, Toronto Ontario, M5S 1A8, Canada.
[3]Department of Pharmaceutical Chemistry, University of Athens, Panepistimiopolis, Athens 157 01, Greece.
[4]Departments of Medicine (Neurology) and Pharmacology, University of Washington, Seattle, Washington 98195.

0277-8068/92/1000-0607$06.50/0

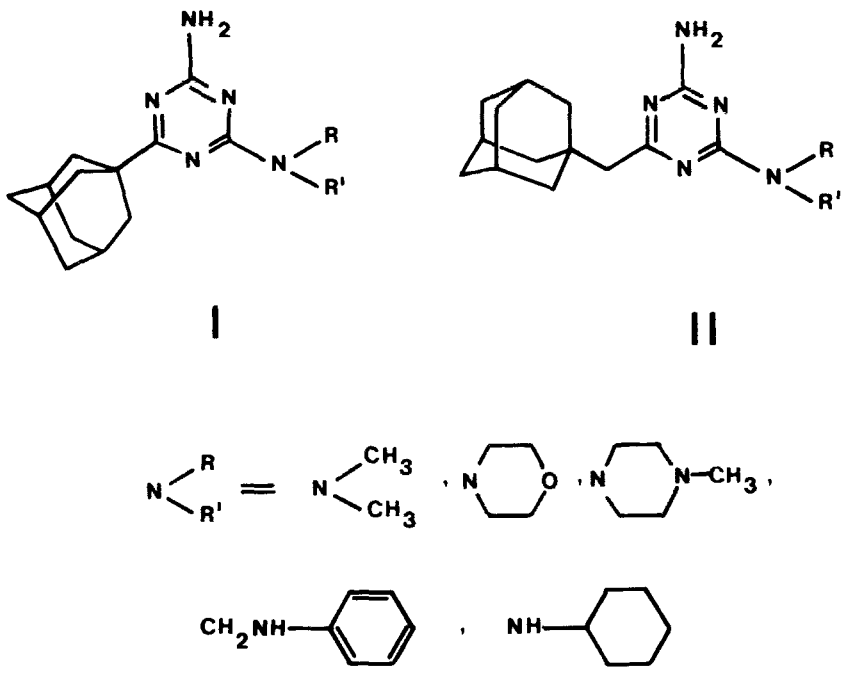

Scheme 1

tal structure determinations and conformational analyses of both active and inactive lipophilic compounds are underway (Hamodrakas *et al.*, in preparation). The title compound is a member of the type I series.

Experimental

Crystals were obtained by evaporation from methanol as thick needles with the needle axis coincident with the space group 3-fold axis. Systematic absences for *hkil*: $-h + k + l = 3n$ indicated the hexagonal system, transformed later to the rhombohedral system of $R3$ space group. The refined cell parameters were obtained by measurement of the angular parameters of 12 high angle reflections ($40 \leq 2\theta \leq 60°$) on a diffractometer and application of the least-squares method.

Crystal data:

hexagonal axis	rhombohedral axis
$a = b = 30.277(11)$ Å	$R3$ space group
$c = 10.132(6)$ Å	$a = b = c = 17.804(9)$ Å
$\gamma = 120°$	$\alpha = \beta = \gamma = 116.48(2)°$
$V = 8043$ Å^3	$V = 2681$ Å^3
$Z = 18$	$Z = 6$

A crystal of dimensions 0.3 × 0.5 × 0.7 mm was chosen for data collection on an automated four-circle diffractometer. Cu $K\alpha$ radiation and $\theta - 2\theta$ scan mode with a scan speed of 2°/min were utilized. Hexagonal axes were chosen to determine the crystal orientation matrix. Three standard reflections monitored every 100 reflections showed only random variations within 5%. A total of 3023 unique reflections were recorded ($3 \leq 2\theta \leq 132°$) of which 1922 were considered observed using $F_o \geq 3\sigma(F_o)$ discrimination. The intensities were corrected for Lorentz and polarization factors. An empirical phi absorption correction was also applied; transmission factor range was 0.88 to 0.99. The cell was then transformed to the rhombohedral system to which all further discussion refers.

The molecular structure was determined by direct methods using SHELXS-86 (Sheldrick, 1985). The E-map with the best figure of merit displayed the triazine and piperazine rings structure, but the adamantyl moiety was disordered. We could interpret the disorder in terms of two distinctly different positions rotated with respect to one another by about 60°. Refinement was carried out by assigning two half-weighted positions each to the three adamantyl carbon atoms attached to C9 and full weighted positions to the other six carbon atoms. Difference maps revealed the positions of all the hydrogen atoms except for those of the adamantyl moiety. Further refinement and difference electron density calculations provided an averaged adamantyl entity with a flattened

six-membered bottom ring, and clearly showed some of the adamantyl hydrogen atoms as well. The discrepancy factor for this solution converged at $R = 6.2\%$.

Because the static disorder of the adamantyl moiety was limited to only two positions related by the rotation of approximately 60° about the C(4)—C(9) bond, it was decided at this point to resolve the averaged structure into two adamantyl moieties using the idealized adamantane molecule, hydrogen atoms included (Donohue and Goodman, 1967) in two distinct conformations. Site occupancy factors for all the atoms of the two adamantyl moieties were fixed at 0.5, except for C9 which has occupancy 1.0. At first a rigid body refinement of the two adamantyl moieties was performed and the R factor at this stage converged at $R = 7\%$. In the next step, restrictions on all atoms of the molecule were relaxed and the structure was subjected to eight cycles of full-matrix refinement, during which the positional parameters of all the atoms including hydrogens were allowed to vary subject to a damping factor of 0.5. The S.O.F. for all the atoms of the two adamantyl moieties were fixed at 0.5. Anisotropic temperature factors for all atoms other than hydrogen were used and allowed to vary, with isotropic temperature factors for H atoms kept constant at $U = 0.07$ Å^2.

The final R-factor converged at 6.1%. The geometry of the two adamantyl moieties, considering the disorder, is reasonable and that of the rest of the molecule is very good, including hydrogens. In this particular case it was very important to start the refinement process from

Table 1. Fractional atomic coordinates and equivalent isotropic temperature factors (U_{eq} = ($U(11) + U(22) + U(33)$)/3) ($\times 10^4$)

Atom	x	y	z	U_{eq} (Å^2)
N1	7659(3)	3809(3)	2862(3)	430
C2	7783(3)	4636(3)	2914(3)	399
N3	6819(3)	4483(3)	2396(3)	396
C4	5674(3)	3413(3)	1828(3)	347
N5	5434(3)	2536(3)	1737(3)	419
C6	6465(3)	2779(3)	2268(3)	391
N7	8987(3)	5723(3)	3555(3)	536
N8	6249(3)	1887(3)	2168(3)	450
C9	4542(3)	3174(3)	1263(3)	381
C10A	4699(5)	3758(5)	2303(5)	530
C11A	4630(5)	3874(5)	930(6)	443
C12A	3054(5)	1568(5)	−202(5)	310
C13A	3575(6)	3527(6)	1775(6)	702
C14A	3660(6)	4222(6)	1470(7)	639
C15A	3477(6)	3616(6)	369(6)	521
C16A	2006(6)	2026(6)	−1010(6)	487
C17A	1900(5)	1323(6)	−746(6)	369
C18A	2099(6)	1927(7)	361(7)	911
C10B	3682(6)	2383(6)	1283(7)	1138
C11B	5217(5)	4610(5)	2235(6)	541
C12B	3581(6)	2338(6)	−191(6)	592
C13B	2460(7)	2069(7)	621(8)	1800
C14B	3181(6)	3505(7)	1606(7)	902
C15B	4044(6)	4337(6)	1627(7)	581
C16B	3120(7)	3504(7)	184(7)	822
C17B	2428(6)	2088(6)	−775(6)	419
C18B	1555(7)	1238(7)	−838(8)	767
C19	7391(3)	2209(3)	2936(3)	511
C20	6800(3)	858(3)	2149(4)	570
N21	5773(3)	1(3)	1921(3)	459
C22	4595(3)	−381(3)	1051(3)	471
C23	5130(3)	946(3)	1819(3)	503
C24	5250(4)	−1274(4)	1237(4)	619

a geometrically idealized adamantyl structure because otherwise the geometry rapidly deteriorates (Donohue and Goodman, 1967). SHELX-76 (Sheldrick, 1976) was used for all refinement calculations, and unit weights were employed. Varying the occupancy parameters for the two adamantyl positions did not lead to an improvement of the *R*-factor.

Discussion

Positional and isotropic thermal parameters of non-hydrogen atoms are listed in Table 1, anisotropic thermal parameters in Table 2, positional parameters for hydrogen atoms in Table 3, and bond lengths and angles in Table 4. A perspective view of the molecule showing the atomic numbering scheme used is given in Fig. 1. A stereoview of the structure, including the hydrogen atoms is presented in Fig. 2.

The orientations of the adamantyl moiety relative to the triazine ring may be described by the torsion angles N3—C4—C9—C11A (21°) and N3—C4—C9—C10B (−155°). Similar orientations have been observed individually in crystal structures of related members of the series (Tsitsa *et al.*, in preparation). Conformational analysis, utilizing semi-empirical INDO energy calculations, showed that rotation of the adamantyl group about the C4—C9 bond does not significantly affect the total molecular energy; thus the observed conformations presumably are stabilized through hydrophobic intermolecular interactions.

Table 2. Anisotropic thermal parameters ($\times 10^4$)

Atom	$U(1, 1)$	$U(2, 2)$	$U(3, 3)$	$U(1, 2)$	$U(1, 3)$	$U(2, 3)$
N1	421(7)	416(7)	454(7)	363(5)	365(5)	347(5)
C2	428(8)	403(7)	369(7)	325(6)	336(6)	337(6)
N3	396(7)	385(7)	407(7)	321(5)	314(5)	312(5)
C4	368(7)	340(7)	335(7)	265(6)	260(6)	291(6)
N5	401(7)	394(7)	464(7)	359(5)	338(5)	333(5)
C6	434(8)	372(7)	369(7)	305(6)	319(6)	338(6)
N7	478(7)	497(7)	634(8)	482(6)	470(6)	410(5)
N8	405(7)	436(7)	512(7)	403(5)	362(5)	353(5)
C9	368(8)	349(7)	427(8)	303(6)	288(6)	289(6)
C10A	499(9)	566(9)	527(9)	429(8)	403(7)	499(7)
C11A	388(9)	390(9)	552(9)	384(7)	317(8)	307(7)
C12A	324(9)	241(9)	368(9)	214(7)	201(8)	189(7)
C13A	503(9)	854(10)	751(9)	626(9)	521(8)	560(8)
C14A	557(10)	578(9)	783(10)	514(9)	489(9)	488(8)
C15A	497(9)	401(9)	667(9)	451(8)	427(8)	360(8)
C16A	355(9)	494(9)	615(9)	458(8)	257(9)	311(8)
C17A	220(9)	326(9)	561(9)	359(7)	211(8)	143(8)
C18A	708(9)	941(9)	1086(10)	906(8)	731(9)	733(8)
C10B	850(9)	1106(9)	1461(10)	1138(8)	1009(8)	875(8)
C11B	520(9)	482(9)	623(9)	444(8)	446(8)	419(7)
C12B	710(9)	655(9)	414(9)	372(8)	348(9)	562(8)
C13B	1290(10)	1573(9)	2538(10)	1905(9)	1658(9)	1346(8)
C14B	620(9)	1154(10)	935(10)	809(9)	661(8)	751(9)
C15B	518(9)	513(9)	714(9)	479(8)	470(8)	454(8)
C16B	762(10)	876(9)	828(10)	692(9)	580(9)	726(8)
C17B	393(10)	503(10)	363(10)	180(9)	72(9)	345(8)
C18B	425(10)	653(10)	1223(10)	590(10)	363(10)	407(9)
C19	429(8)	501(8)	604(8)	462(6)	411(6)	401(6)
C20	580(8)	525(8)	606(8)	483(6)	501(6)	481(6)
N21	527(7)	410(7)	441(7)	360(5)	391(5)	397(5)
C22	472(8)	443(8)	500(8)	392(6)	367(6)	371(6)
C23	455(8)	467(8)	589(8)	454(6)	416(6)	390(6)
C24	756(8)	506(8)	596(8)	445(6)	543(6)	541(6)

Table 3. Hydrogen atom coordinates ($\times 10^4$)

Atom	x	y	z	Atom	x	y	z
H3A	3668	4016	2496	H21B	3041	1275	−944
H5A	3569	4100	138	H22B	4122	2866	−271
H7A	893	203	−1742	H41B	2474	3402	1259
H01A	5714	4881	3352	H42B	3977	4184	2710
H02A	4609	3348	2540	H61B	3670	4084	171
H11A	5682	4969	1903	H62B	2291	3317	−215
H12A	4543	3427	159	H81B	752	1089	−1217
H21A	2975	1134	14	H82B	1054	244	−1515
H22A	2942	1092	−871	H71	9638	5818	3880
H41A	2848	4023	1051	H72	9153	6329	3680
H42A	4685	5344	2417	H191	8070	2767	3076
H61A	1897	1559	−1810	H192	7992	2845	3962
H62A	1206	1817	−1434	H201	6343	313	1217
H81A	1279	1719	−34	H202	7581	1083	2716
H82A	2015	1485	525	H221	3861	−1010	904
H3B	1962	1591	654	H222	4075	−1038	32
H5B	4572	5359	2379	H231	4346	694	1160
H7B	1643	1468	−1864	H232	5568	1518	2796
H01B	4387	2985	2291	H241	6023	−1029	1790
H02B	3166	1351	582	H242	4584	−1786	1163
H11B	5958	5218	3283	H243	4760	−1911	302
H12B	5807	5168	2240				

Table 4. Bond lengths (Å)

N1	C6	1.338	C9	C10B	1.582
N1	C2	1.339	C10B	C13B	1.564
C2	N7	1.338	C11B	C15B	1.542
C2	N3	1.348	C12B	C17B	1.536
N3	C4	1.336	C13B	C18B	1.506
C4	N5	1.329	C13B	C14B	1.527
C4	C9	1.517	C14B	C15B	1.558
N5	C6	1.353	C15B	C16B	1.479
C6	N1	1.338	C16B	C17B	1.519
C6	N8	1.357	C17B	C18B	1.516
N8	C19	1.454			
N8	C23	1.465			
C19	C20	1.509			
C20	N21	1.459			
N21	C24	1.463			
N21	C22	1.467			
C22	C23	1.520			
C10A	C9	1.468			
C10A	C13A	1.522			
C11A	C15A	1.530			
C11A	C9	1.580			
C12A	C17A	1.548			
C12A	C9	1.558			
C13A	C14A	1.533			
C13A	C18A	1.545			
C14A	C15A	1.526			
C15A	C16A	1.533			
C16A	C17A	1.491			
C17A	C18A	1.526			
C9	C4	1.517			
C9	C12B	1.475			
C9	C11B	1.560			

Bond angles (°)

C6	N1	C2	114.04
N7	C2	N1	116.42
N7	C2	N3	117.35
N1	C2	N3	126.23
C4	N3	C2	113.73
N5	C4	N3	126.05
N5	C4	C9	115.43
N3	C4	C9	118.50
C4	N5	C6	114.71
N1	C6	N5	125.20
N1	C6	N8	118.12
N5	C6	N8	116.68
C6	N8	C19	120.82
C6	N8	C23	120.22
C19	N8	C23	114.22
N8	C19	C20	110.08
N21	C20	C19	110.35
C20	N21	C24	111.30
C20	N21	C22	109.10

Table 4. Continued

Bond angles (°)							
C24	N21	C22	110.21	C4	C9	C12A	109.63
N21	C22	C23	109.93	C4	C9	C11A	111.66
N8	C23	C22	109.47	C12A	C9	C11A	103.87
C9	C10A	C13A	110.78	C12B	C9	C11B	109.88
C15A	C11A	C9	110.05	C12B	C9	C10B	110.03
C17A	C12A	C9	109.36	C11B	C9	C10B	106.03
C10A	C13A	C14A	110.86	C13B	C10B	C9	109.47
C10A	C13A	C18A	109.04	C15B	C11B	C9	109.82
C14A	C13A	C18A	107.09	C9	C12B	C17B	110.65
C15A	C14A	C13A	110.15	C18B	C13B	C14B	111.76
C14A	C15A	C11A	108.68	C18B	C13B	C10B	109.14
C14A	C15A	C16A	108.73	C14B	C13B	C10B	106.52
C11A	C15A	C16A	110.56	C13B	C14B	C15B	109.58
C17A	C16A	C15A	109.12	C16B	C15B	C11B	108.84
C16A	C17A	C18A	109.80	C16B	C15B	C14B	109.96
C16A	C17A	C12A	110.34	C11B	C15B	C14B	108.81
C18A	C17A	C12A	109.06	C15B	C16B	C17B	110.93
C17A	C18A	C13A	110.14	C18B	C17B	C16B	110.76
C10A	C9	C4	109.01	C18B	C17B	C12B	108.50
C10A	C9	C12A	112.43	C16B	C17B	C12B	109.48
C10A	C9	C11A	110.21	C13B	C18B	C17B	109.94

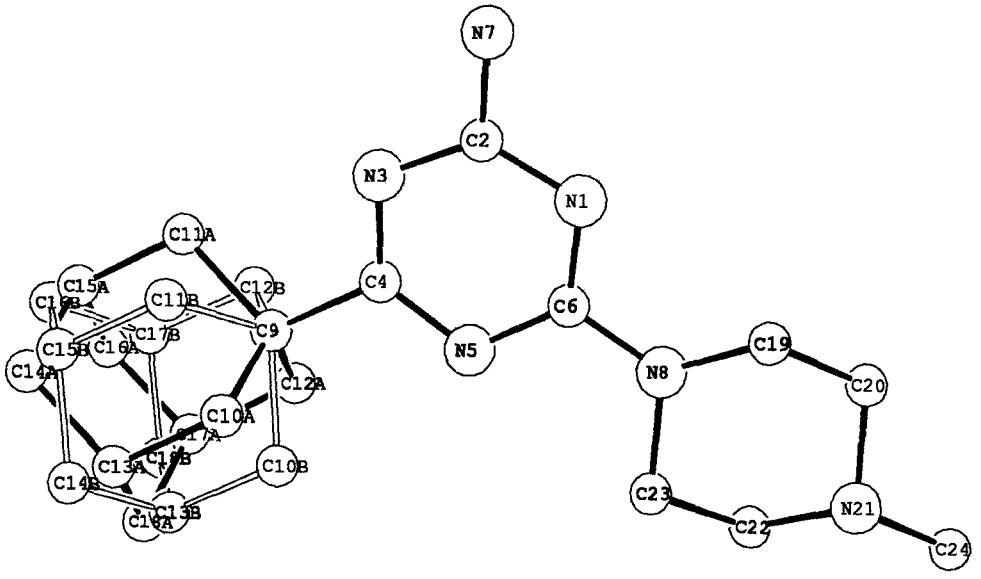

Fig. 1. The numbering scheme.

The adamantyl substitution at position 4 does not affect the triazine ring planarity (maximum deviation of ring atoms from the least squares plane of the triazine is 0.01 Å.). The piperazine ring adopts the usual chair conformation, with N(8) and N(21) above and below the C(19), C(20), C(22), C(23) plane by 0.6 and 0.7 Å respectively. The two rings are approximately coplanar; the angle between normals to the plane of the triazine ring and the best plane through the six atoms of the piperazine ring is 11°.

The crystal structure and molecular packing is illustrated in Fig. 3. There is a hydrogen bond between the N(7) amino group and N(21) of the piperazine ring of another molecule; distances N(7) · · · N(21) and

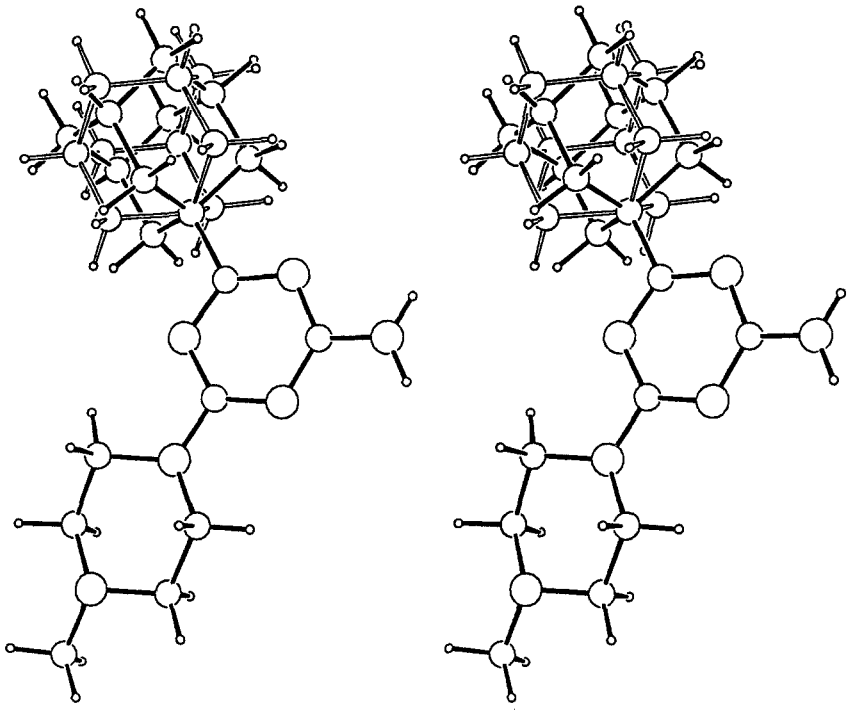

Fig. 2. Stereodiagram of the molecular structure.

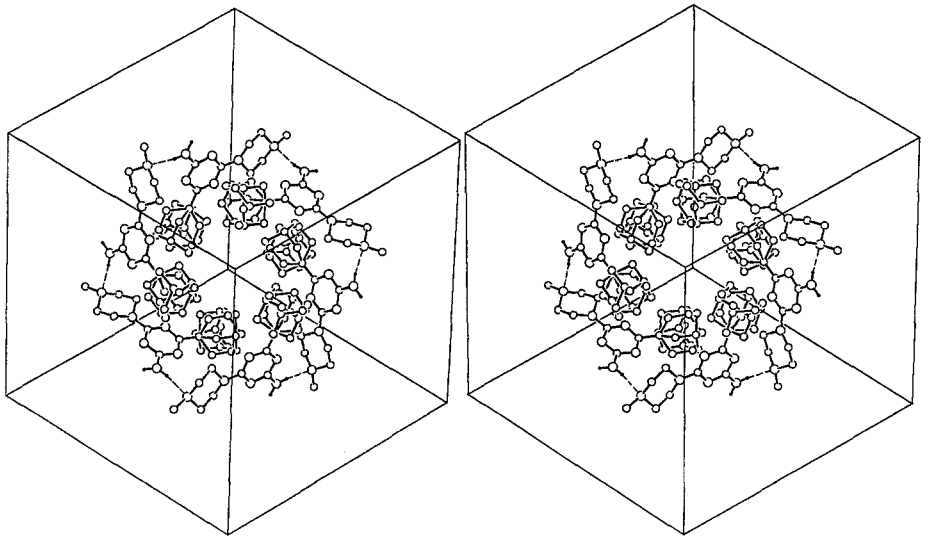

Fig. 3. Stereodiagram of the hexamer.

H72 · · · N(21) are 3.02 and 2.17 Å and the N(7)—H72 · · · N(21) angle is 168°. The consequence of this intermolecular interaction in the rhombohedral space group is to arrange the molecules into hexamers. The triazine/piperazine ring systems of six molecules form the edges of a cube with the adamantyl groups occupying (roughly) the center of each cube face. The hexamers are arranged in stacks along the crystallo-

graphic three fold axes; this mode of hexamer stacking provides for hydrophobic channels, bounded by the adamantyl groups, running along the threefold axes. There are only van der Waals interactions between the hexamers.

References

Antoniadou-Vyzas, A., and Foscolos, G. B. (1986) *Eur. J. Med. Chem.* **21,** 73–74.

Baccarani, D. P., Daluge, S., and King, R. W. (1982) *Biochemistry.* **21,** 5068–5075.

Blakley, R. L. (1969) *The biochemistry of folic acid and related pteridines* (Frontiers in Biology, 13), North Holland, Amsterdam.

Donohue, J., and Goodman, S. H. (1967) *Acta Crystallogr.* **22,** 352–354.

Garoufalias S., Vyzas, A., Fytas, G., Foscolos, G. B., and Chytiroglou, A. (1988) *Ann. Pharm. Francaises.* **46,** 97–104.

Greco, W. R., and Hakala, M. T. (1980) *J. Pharmacol. Exp. Ther.* **212,** 39–41.

Hitchings, G. H., and Smith, S. L. (1980) *Adv. Enzyme Regul.* **18,** 349–371.

Modest, E. J., Foley, G. E., Pechet, M. U., and Farber, S. (1952) *J. Am. Chem. Soc.* **74,** 855–857.

Sheldrick, G. M. (1976) SHELX*76 Program for crystal structure determination*, (University of Cambridge, England).

Sheldrick, G. M. (1985) in *Crystallographic computing 3* G. M. Sheldrick, C. Kruger, and R. Goddard, (eds.) (Oxford University Press), pp. 175–189.

Structure factor data have been deposited with the British Library, Boston Spa, Wetherby, West Yorkshire, UK, as supplementary publication No. 67089 (10 pages).